

## Magnetization dynamics induced by in-plane currents in ultrathin magnetic nanostructures with Rashba spin-orbit coupling

Kyoung-Wan Kim,<sup>1</sup> Soo-Man Seo,<sup>2</sup> Jisu Ryu,<sup>1</sup> Kyung-Jin Lee,<sup>2,3,4,\*</sup> and Hyun-Woo Lee<sup>1,†</sup>

<sup>1</sup>Center for Theoretical Physics (PCTP) and Department of Physics, Pohang University of Science and Technology, Pohang 790-784, Korea

<sup>2</sup>Department of Materials Science and Engineering, Korea University, Seoul 136-701, Korea

<sup>3</sup>Center for Nanoscale Science and Technology, National Institute of Standards and Technology, Gaithersburg, Maryland 20899-8412, USA

<sup>4</sup>Maryland Nanocenter, University of Maryland, College Park, Maryland 20742, USA

(Received 16 November 2011; revised manuscript received 24 April 2012; published 8 May 2012)

Recent experiments on ultrathin magnetic layers with broken inversion symmetry reported anomalous current-driven magnetization dynamics. We show that the spin-transfer torque can be significantly modified by Rashba spin-orbit coupling and the modified spin-transfer torque can explain the anomalous magnetization dynamics. This work will be valuable for the development of next generation spintronic devices based on ultrathin magnetic systems.

DOI: [10.1103/PhysRevB.85.180404](https://doi.org/10.1103/PhysRevB.85.180404)

PACS number(s): 75.70.Tj, 72.25.Ba, 75.76.+j, 75.78.Fg

Electric control of magnetic states carries a high potential toward device applications<sup>1,2</sup> such as magnetic memory and logic. Spin-transfer torque (STT)<sup>3,4</sup> arising from a spin-polarized current is an efficient way to achieve electric control in magnetic nanostructures. There have been extensive efforts to clarify the properties of STT and enhance the efficiencies of STT both theoretically<sup>5–10</sup> and experimentally.<sup>11–13</sup>

Recently the current-driven magnetization dynamics of ultrathin ( $\lesssim 1$  nm) magnetic layers has received considerable attention.<sup>14</sup> In particular, experiments<sup>15,16</sup> on an ultrathin (0.6 nm) magnetic layer (Co) sandwiched between a heavy metal layer (Pt) and an oxide layer (AlO<sub>x</sub>) (Fig. 1) revealed a number of anomalous features: (i) When an in-plane current is supplied to the system, a domain wall (DW) in the ultrathin magnetic layer moves *against* the electron flow direction,<sup>16,17</sup> which is in clear contrast to STT theories<sup>9</sup> predicting DW motion *along* the electron flow direction. (ii) DW moves at speeds as high as 400 m/s.<sup>16</sup> This is about four times higher than the highest speed of current-driven DW motion reported previously.<sup>13</sup> The origin of the speed enhancement is not clear. (iii) When an external magnetic field is applied parallel to the in-plane current, the in-plane current induces the magnetization switching of the magnetic layer in a single domain state.<sup>15</sup> Recalling that the trilayer system does not contain a second magnetic layer, this result is again at odds with STT theories,<sup>3</sup> which require a second magnetic layer for current-driven magnetization switching. These anomalies imply that this ultrathin magnetic system is not a mere thin limit of thicker counterparts but is a qualitatively different system governed by different physics. A clear understanding of its core physics will be highly valuable for the development of powerful spintronic devices; higher DW speed implies faster device operation, and switching by an in-plane current opens a possibility to lower the switching energy since the cross-sectional area for an in-plane current can be orders of magnitude smaller than that for a perpendicular current, providing room for the reduction of the switching current threshold.

An experiment<sup>18</sup> reported that conduction electrons in a trilayer system are subject to Rashba spin-orbit coupling (RSOC). The emergence of RSOC (Ref. 19) is reasonable in

this ultrathin magnetic layer since its upper and lower layers are made of quite different materials (Fig. 1), breaking the structural symmetry, and the magnetic layer being ultrathin makes the layer more susceptible to symmetry breaking effects. Motivated by this report,<sup>18</sup> we explore the possible relations between RSOC and the anomalies. Previous theoretical studies<sup>20,21</sup> reported that RSOC generates a contribution to STT that is proportional to  $-\alpha_R \mathbf{m} \times (\hat{\mathbf{z}} \times \mathbf{j}_e)$ , which should be added to conventional STT (Ref. 9) in the absence of RSOC. Here  $\alpha_R$  is the parameter describing the strength of RSOC,  $\mathbf{j}_e$  is the in-plane current density in the ultrathin magnetic layer,  $\hat{\mathbf{z}}$  is the unit vector perpendicular to the layer, and  $\mathbf{m}$  is the unit vector along the magnetization in the ultrathin magnetic layer. Since this contribution has the same structure as the field torque ( $\propto -\mathbf{m} \times \mathbf{H}$ ), we call it fieldlike STT (FL-STT) arising from an effective field  $\propto \alpha_R \hat{\mathbf{z}} \times \mathbf{j}_e$ . FL-STT, however, cannot explain anomalies (i) and (ii), as we demonstrated recently.<sup>22</sup>

Here we demonstrate theoretically that when RSOC is combined with electron scattering, it generates still another contribution to STT that is proportional to  $\beta \alpha_R \mathbf{m} \times [\mathbf{m} \times (\hat{\mathbf{z}} \times \mathbf{j}_e)]$ ,<sup>23</sup> where the nonadiabaticity parameter  $\beta$  is a measure of the scattering-induced spin-relaxation rate of conduction electrons. This contribution has the same structure as the Slonczewski STT (Ref. 3) [ $\propto I \mathbf{m} \times (\mathbf{m} \times \mathbf{P})$ ] generated by a *perpendicular* current  $I$  in a vertically stacked magnetic nanostructure containing two magnetic layers, with their magnetization directions given by  $\mathbf{m}$  and  $\mathbf{P}$ , respectively. This structural similarity motivates us to call it Slonczewski-like STT (SL-STT). To understand the implications of SL-STT for anomaly (iii), it is useful to interpret SL-STT as a torque arising from the effective field  $-\beta \alpha_R \mathbf{m} \times (\hat{\mathbf{z}} \times \mathbf{j}_e) = -\beta \alpha_R [(\mathbf{m} \cdot \mathbf{j}_e) \hat{\mathbf{z}} - (\mathbf{m} \cdot \hat{\mathbf{z}}) \mathbf{j}_e]$ . Recalling that the system in the switching experiment<sup>15</sup> has perpendicular magnetic anisotropy (PMA), the first term of the effective field is either parallel or antiparallel to the effective field due to PMA. When it is antiparallel and strong enough to overcome PMA, it can switch the  $z$  component of  $\mathbf{m}$ , explaining anomaly (iii). To make its magnitude  $\beta \alpha_R (\mathbf{m} \cdot \mathbf{j}_e)$  large,  $\mathbf{j}_e$  (along the  $x$  direction) should be large and  $\mathbf{m}$  should be forced to acquire a sufficient  $x$  component by applying an external magnetic field. By the way, the second term of the effective field is orthogonal to

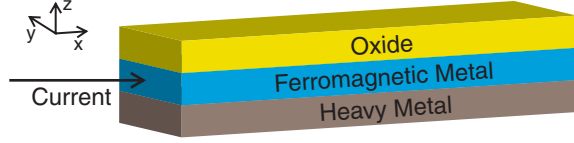


FIG. 1. (Color online) Schematic structure. An ultrathin ( $\lesssim 1$  nm) magnetic layer is sandwiched between a heavy metallic layer and an insulating oxide layer.

the PMA direction and is not crucial for the switching. Below we first derive SL-S TT and then show that SL-S TT explains anomalies (i) and (ii) as well when combined with FL-S TT.

The derivation of SL-S TT goes as follows. We add the RSOC Hamiltonian  $H_{\text{RSOC}} = (\alpha_{\text{R}}/\hbar)(\sigma_{\text{op}} \times \mathbf{p}_{\text{op}}) \cdot \hat{\mathbf{z}}$  to the conventional  $s$ - $d$  Hamiltonian<sup>6,7,9</sup> to obtain the total Hamiltonian  $H$  describing conduction electrons in an ultrathin magnetic layer subject to RSOC,

$$H = \frac{\mathbf{p}_{\text{op}}^2}{2m_e} + J_{\text{ex}}\sigma_{\text{op}} \cdot \mathbf{m} + H_{\text{rel}} + H_{\text{RSOC}}, \quad (1)$$

where  $\mathbf{p}_{\text{op}}$  is the momentum operator,  $m_e$  is the electron mass,  $J_{\text{ex}} (>0)$  is the exchange energy,  $\sigma_{\text{op}}$  is the Pauli spin operator, and  $H_{\text{rel}}$  describes electron scattering responsible for spin relaxation. Note that  $\mathbf{m}$  appears only as a *classical* vector field in  $H$ . Since S TT arises when the local spin direction of conduction electrons deviates from  $\pm \mathbf{m}$ ,<sup>9</sup> evaluation of the deviation in the presence of RSOC is the central part of this derivation.

Since conduction electron dynamics is much faster than magnetization dynamics, the time dependence of  $\mathbf{m}$  may be ignored in the leading approximation. Corrections to this approximation will be presented below. Then the many-body nonequilibrium state describing current-carrying conduction electrons can be constructed by filling up the eigenstates of the time-independent single-particle Hamiltonian  $H$ , following the Landauer-Büttiker description<sup>24</sup> of electron transport. To evaluate the local spin density of this many-body state, it is useful to note that the strong exchange energy  $J_{\text{ex}}$ , which is the largest energy scale affecting the conduction electron spin dynamics in conventional metallic ferromagnets (including Co), allows one to classify eigenstates of  $H$  into two groups, majoritylike and minoritylike states. Each group generates the local spin density  $\mathbf{s}_{\pm}(\mathbf{r}) \equiv \langle \sigma_{\text{op}} \delta(\mathbf{r}_{\text{op}} - \mathbf{r}) \rangle_{\pm}$ , where  $\mathbf{r}_{\text{op}}$  is the position operator and  $\langle \cdot \rangle_{\pm}$  denotes the sum over expectation values over all occupied majoritylike/minoritylike states. The sum  $\mathbf{s}(\mathbf{r}) \equiv \mathbf{s}_{+}(\mathbf{r}) + \mathbf{s}_{-}(\mathbf{r})$  determines the total local spin density. To evaluate  $\mathbf{s}_{\pm}(\mathbf{r})$ , it is convenient to derive an equation that it satisfies. From the spin continuity equation determined by  $H$ , we obtain the Bloch equation

$$\nabla \cdot \mathcal{J}_{\pm} = -\frac{\mathbf{s}_{\pm}}{\tau_{\text{ex}}} \times \left[ \mathbf{m} + \frac{2\alpha_{\text{R}}m_e\tau_{\text{ex}}}{\hbar^2}(\mathbf{v}_{\pm} \times \hat{\mathbf{z}}) \right] + \langle \Gamma \rangle_{\pm}, \quad (2)$$

where  $\tau_{\text{ex}} = \hbar/2J_{\text{ex}}$ ,  $\Gamma = [\sigma_{\text{op}}, H_{\text{rel}}]/i\hbar$ , and the spin-current tensor density  $\mathcal{J}_{\pm} = \mathbf{v}_{\pm} \otimes \mathbf{s}_{\pm}$ . Here  $\mathbf{v}_{\pm}$  is the average expectation value of the kinematic velocity operator  $\mathbf{v}_{\text{op}} \equiv \mathbf{p}_{\text{op}}/m_e + (\alpha_{\text{R}}/\hbar)\hat{\mathbf{z}} \times \sigma_{\text{op}}$  over occupied majoritylike/minoritylike states. In deriving Eq. (2),  $\langle \{(\sigma_{\text{op}})_i(\mathbf{v}_{\text{op}})_j, \delta(\mathbf{r}_{\text{op}} - \mathbf{r})\} + \{(\mathbf{v}_{\text{op}})_j(\sigma_{\text{op}})_i, \delta(\mathbf{r}_{\text{op}} - \mathbf{r})\} \rangle_{\pm}$  is approximated by  $4[\mathbf{s}_{\pm}(\mathbf{r})]_i(\mathbf{v}_{\pm})_j$ . Equation (2) uniquely fixes

$\mathbf{s}_{\pm}(\mathbf{r})$  as a function of  $\mathbf{m}$  and  $\mathbf{v}_{\pm}$ , where  $\mathbf{v}_{\pm}$  carries the current dependence of  $\mathbf{s}_{\pm}$ . It is convenient to separate  $\mathbf{s}_{\pm}$  into longitudinal and transverse components,  $\mathbf{s}_{\pm} = (\mathbf{s}_{\pm} \cdot \mathbf{m})\mathbf{m} + \delta\mathbf{s}_{\pm}$ , since for large  $J_{\text{ex}}$ , the longitudinal component is essentially independent of current and  $n_{\pm} \equiv \mp \mathbf{s}_{\pm} \cdot \mathbf{m}$  may be identified as the majority/minority number density of conduction electrons. One then makes the relaxation time approximation<sup>9</sup>  $\langle \Gamma \rangle_{\pm} = -\delta\mathbf{s}_{\pm}/\tau_{\text{sr}}$ , where  $\tau_{\text{sr}}$  is the transverse spin relaxation time. In this approximation, the relaxation of the longitudinal spin component is neglected since the transverse relaxation is much faster in conventional metallic ferromagnets and also the longitudinal spin component does not affect S TT. From Eq. (2), one then obtains

$$\delta\mathbf{s}_{\pm} = \pm n_{\pm}\tau_{\text{ex}} \frac{(\beta + \mathbf{m} \times)}{1 + \beta^2} \left[ D^{\pm}\mathbf{m} + \frac{2\alpha_{\text{R}}m_e}{\hbar^2}\mathbf{m} \times (\mathbf{v}_{\pm} \times \hat{\mathbf{z}}) \right], \quad (3)$$

where  $\beta = \tau_{\text{ex}}/\tau_{\text{sr}}$  and  $D^{\pm} = \mathbf{v}_{\pm} \cdot \nabla$ . We remark that when the time dependence of  $\mathbf{m}$  is taken into account, the left-hand side of Eq. (2) acquires an additional term  $\partial\mathbf{s}_{\pm}/\partial t$  and  $D^{\pm}$  in the above equation is replaced by  $\partial_t + \mathbf{v}_{\pm} \cdot \nabla$ . Then Eq. (2) becomes the RSOC generalization of the Bloch equation in Ref. 9 without RSOC.

Finally from the relation  $\mathbf{T} = \mu_B\tau_{\text{ex}}^{-1}\mathbf{m} \times \mathbf{s}$  (Ref. 9) between the total S TT  $\mathbf{T}$  and  $\mathbf{s}$ , one obtains the Landau-Lifshitz-Gilbert (LLG) equation  $\partial\mathbf{M}/\partial t = -\gamma_0\mathbf{M} \times \mathbf{H}_{\text{eff}} + (\alpha_0/M_s)\mathbf{M} \times \partial\mathbf{M}/\partial t + \mathbf{T}$ , where  $\mathbf{H}_{\text{eff}}$  is a sum of an external magnetic field and effective magnetic fields due to magnetic anisotropy and magnetic exchange energy.  $\mathbf{M} = M_s\mathbf{m}$  is the magnetization and  $M_s$  is the saturation magnetization in the ultrathin magnetic layer. After grouping together terms of the same structure, one obtains

$$\begin{aligned} \frac{\partial\mathbf{M}}{\partial t} = & -\gamma\mathbf{M} \times \left( \mathbf{H}_{\text{eff}} + \mathbf{H}_{\text{R}} - \frac{\beta}{M_s}\mathbf{M} \times \mathbf{H}_{\text{R}} \right) \\ & + \frac{\alpha}{M_s}\mathbf{M} \times \frac{\partial\mathbf{M}}{\partial t} + \frac{\mu_B P}{eM_s(1 + \beta^2)}(\mathbf{j}_e \cdot \nabla)\mathbf{M} \\ & - \frac{\beta\mu_B P}{eM_s^2(1 + \beta^2)}\mathbf{M} \times (\mathbf{j}_e \cdot \nabla)\mathbf{M}, \end{aligned} \quad (4)$$

$$\mathbf{H}_{\text{R}} = \frac{\alpha_{\text{R}}m_e P}{\hbar eM_s(1 + \beta^2)}(\hat{\mathbf{z}} \times \mathbf{j}_e), \quad (5)$$

where  $\mathbf{H}_{\text{R}}$  is the additional effective field due to RSOC,  $\mathbf{j}_e = -e(n_+\mathbf{v}_+ + n_-\mathbf{v}_-)$ ,<sup>25</sup> and  $P\mathbf{j}_e = -e(n_+\mathbf{v}_+ - n_-\mathbf{v}_-)$ . Note that the first and fourth terms on the right-hand side of Eq. (4) contain the renormalized gyromagnetic ratio  $\gamma$  and the renormalized Gilbert damping  $\alpha$  given by  $\gamma_0/\gamma = 1 + (n_+ - n_-)/[M_s(1 + \beta^2)]$ , and  $\gamma\alpha/\gamma_0 = \alpha_0 + \beta(n_+ - n_-)/[M_s(1 + \beta^2)]$ . The last and second to the last terms are the nonadiabatic S TT (Refs. 9 and 10) and the adiabatic S TT.<sup>6</sup> When  $\alpha_{\text{R}}$  is set to zero, Eq. (4) reduces to the LLG equation obtained for thicker magnetic systems.<sup>9</sup>

RSOC effects are contained in the second and third terms. The second term is FL-S TT, which has been derived before,<sup>20,21</sup> and the third term is SL-S TT, whose derivation is one of main results of this Rapid Communication. Note that SL-S TT does not contain any space derivative, which is in contrast to the nonadiabatic S TT (Ref. 9) being proportional to space derivative of  $\mathbf{m}$ . Considering that both S TTs

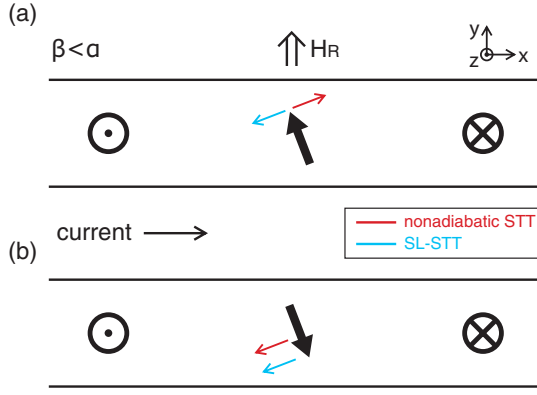


FIG. 2. (Color online) Two possible structures of a Bloch-type transverse DW in a PMA system when a current flows to the right and  $\alpha > \beta$  (Ref. 26). Thick and thin arrows represent the directions of  $\mathbf{m}$  and STTs, respectively. Note that the direction of  $\mathbf{m}$  deviates from  $\pm\hat{y}$ , which is a generic feature of a moving DW (Refs. 9 and 10) with  $\alpha \neq \beta$ .

arise from electron-scattering-induced spin relaxation and are proportional to  $\beta$ , this difference is worth clarifying. In the absence of RSOC, the effective magnetic field acting on conduction electrons is just  $J_{\text{ex}}\mathbf{m}$ . Thus when  $\mathbf{m}$  is uniform, conduction electrons are subject to a constant effective field and  $\mathbf{s}_{\pm}$  should be aligned with  $\mp\mathbf{m}$  regardless of  $\beta$ . Hence  $\mathbf{m}$  should not be uniform for  $\beta$  to play any role. If  $\alpha_R \neq 0$ , on the other hand, the effective magnetic field acting on conduction electrons becomes  $J_{\text{ex}}\mathbf{m} + (\alpha_R/\hbar)\mathbf{p}_{\text{op}} \times \hat{z}$ , which depends on  $\mathbf{p}_{\text{op}}$  and is forced to fluctuate by electron scattering. Thus even when  $\mathbf{m}$  is uniform, conduction electrons feel a varying effective field and  $\mathbf{s}_{\pm}$  depends on  $\beta$ . This explains why SL-STT can survive even when  $\mathbf{m}$  is uniform.

Next we demonstrate the implications of FL-STT and SL-STT on anomalies (i) and (ii). We begin with two possible structures of a Bloch-type transverse DW (Fig. 2) in ultrathin magnetic systems<sup>16</sup> with PMA. Without RSOC, the two structures are equivalent in term of both stability and dynamics (the same DW velocity  $v_{\text{DW}}$ ). The first effect of RSOC is to break the dynamic equivalence; at the DW center in Fig. 2(a) [Fig. 2(b)], SL-STT is antiparallel (parallel) to the nonadiabatic STT, effectively cancelling (enlarging) the effect of the nonadiabatic STT. Recalling that the nonadiabatic STT determines  $v_{\text{DW}}$ ,<sup>9,10</sup> this implies that SL-STT reduces (increases)  $v_{\text{DW}}$ . When RSOC is sufficiently strong, it is even possible for SL-STT to overcancel the nonadiabatic STT in Fig. 2(a), so that  $v_{\text{DW}}$  reverses its sign. When RSOC is even stronger, the DW in Fig. 2(a) moves *fast against* the electron flow direction. By the way, FL-STT does not affect  $v_{\text{DW}}$  (Ref. 22) since it is perpendicular to the nonadiabatic STT at the DW center. The second effect of RSOC is to break the stability equivalence. The effect of FL-STT on the stability can be understood from the direction of the effective field  $\mathbf{H}_R$ . Since the effective energy density  $-\mathbf{H}_R \cdot \mathbf{M}$  is negative (positive) at the DW center for the DW structure in Fig. 2(a) [Fig. 2(b)], FL-STT makes the DW structure in Fig. 2(a) more stable than the other. When  $\mathbf{H}_R$  is sufficiently strong, the DW structure in Fig. 2(b) becomes unstable and evolves to the stable DW structure in Fig. 2(a).<sup>22</sup> Incidentally, SL-STT has

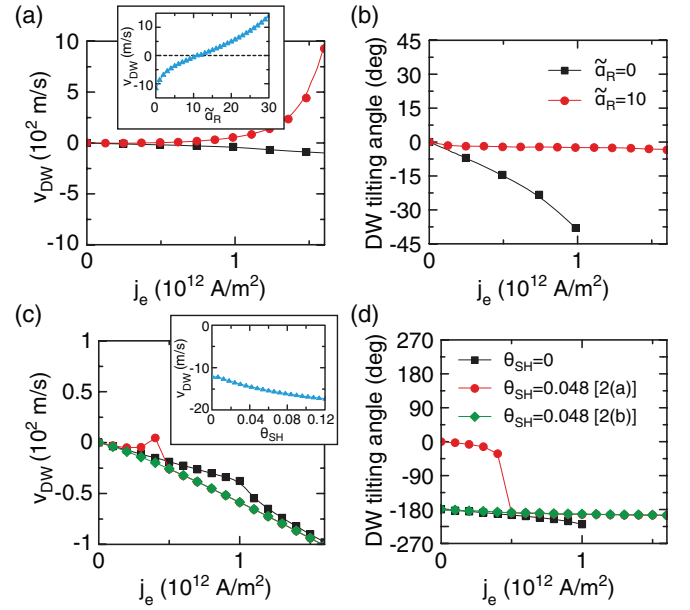


FIG. 3. (Color online) Micromagnetic simulation results of the current-driven DW motion. In (a) and (b), RSOC effects are examined by using Eq. (4). (a)  $v_{\text{DW}}$  as a function of  $\tilde{\alpha}_R$  for  $j_e = 3.0 \times 10^{11}$  A/m<sup>2</sup> (inset) and as a function of  $j_e$  for  $\tilde{\alpha}_R = 0$  (black squares) and  $\tilde{\alpha}_R = 10$  (red circles). (b) DW tilting angle  $\phi$  (measured clockwise from the  $+\hat{y}$  direction in Fig. 2) indicates that the Walker breakdown is suppressed by FL-STT if  $\tilde{\alpha}_R = 10$  and occurs for  $j_e > 1.0 \times 10^{12}$  A/m<sup>2</sup> if  $\tilde{\alpha}_R = 0$ . In (c) and (d), SHE effects are examined by setting  $\mathbf{H}_R = 0$  and instead adding to Eq. (4) the SHE-induced Slonczewski STT  $\gamma\mathbf{M} \times [(\theta_{\text{SH}}\mathbf{M}/M_s) \times (H_s\hat{y})]$  (Ref. 27), where  $\theta_{\text{SH}}$  is the spin Hall angle,  $H_s = \hbar j_{e,N}/(2eM_s t_F)$ ,  $t_F$  is the thickness of the ultrathin magnetic layer, and  $j_{e,N} = j_e$  is assumed.  $v_{\text{DW}}$  (c) and  $\phi$  (d) as a function of  $j_e$  for  $\theta_{\text{SH}} = 0$  (black squares) and 0.048 [red circles and green diamonds for the DW structures in Figs. 2(a) and 2(b)]. Red circles are not visible for  $j_e > 5 \times 10^{11}$  A/m<sup>2</sup> since the corresponding DW structure in Fig. 2(a) becomes unstable. The inset in (c) shows  $v_{\text{DW}}$  as a function of  $\theta_{\text{SH}}$  at  $j_e = 3.0 \times 10^{11}$  A/m<sup>2</sup> for the stable DW structure in Fig. 2(b). The parameters for the simulation are as follows:  $\alpha = 0.5$ ,  $\beta = 0.25$  (Ref. 26),  $M_s = 5.0 \times 10^5$  A/m, the PMA constant  $K_u = 1.0 \times 10^6$  J/m<sup>3</sup>, the exchange stiffness constant  $A_{\text{ex}} = 1.0 \times 10^{-11}$  J/m,  $P = 0.7$ ,  $\gamma/2\pi = 28.0113$  GHz T<sup>-1</sup>, and  $t_F = 0.6$  nm.

a weaker effect on the stability than FL-STT since, according to Eq. (4), SL-STT is smaller than FL-STT in magnitude by a factor  $\beta$ , which is usually smaller than 1.<sup>9,26</sup> Then combining the above information, we find that there is only one stable DW structure [Fig. 2(a)] when RSOC is sufficiently strong and that it moves fast against the electron flow direction, explaining both anomalies (i) and (ii).

Figures 3(a) and 3(b) show the micromagnetic simulation results of Eq. (4) for the stable DW structure in Fig. 2(a). Various parameter values used in the simulation are given in the caption of Fig. 3. The inset in Fig. 3(a) shows  $v_{\text{DW}}$  as a function of a dimensionless parameter  $\tilde{\alpha}_R \equiv \pi\alpha_R m_e \lambda/\hbar^2$  at fixed  $j_e \equiv \hat{x} \cdot \mathbf{j}_e = +3 \times 10^{11}$  A/m<sup>2</sup>, where  $\lambda$  is the DW width at  $j_e = 0$ . Note that as  $\tilde{\alpha}_R$  increases,  $v_{\text{DW}}$  changes its sign from negative (along the electron flow direction) to positive (against the electron flow direction). The main panel in Fig. 3(a) shows

$v_{\text{DW}}$  as a function of  $j_e$  at two fixed values of  $\tilde{\alpha}_R$ , 0 (black squares) and 10 (red circles). For  $\tilde{\alpha}_R = 10$ ,  $v_{\text{DW}}$  changes from negative to positive at  $j_e \approx 3.5 \times 10^{11}$  A/m<sup>2</sup> and goes above +500 m/s for  $j_e > 1.5 \times 10^{12}$  A/m<sup>2</sup>. Thus both anomalies (i) and (ii) can be explained by RSOC if  $\tilde{\alpha}_R$  is sufficiently larger than 1. For the value of  $\alpha_R = 10^{-10}$  eV m (Ref. 18) reported for Pt/Co(0.6 nm)/AlO<sub>x</sub>,  $\tilde{\alpha}_R$  becomes 13 if we assume  $\lambda = 3$  nm. The results for the DW structure in Fig. 2(b) are not shown since, when  $\tilde{\alpha}_R = 10$ , it is unstable for  $j_e > 7.4 \times 10^{10}$  A/m<sup>2</sup>.

Lastly, to utilize the RSOC effects for device applications, it is desired to understand when  $\alpha_R$  becomes large. In the case of a normal metal in contact with a heavy metal, there are well-known material combinations<sup>28,29</sup> generating large  $\alpha_R$  in the range  $(0.4-3) \times 10^{-10}$  eV m for conduction electrons near the interface. In comparison, to the best of our knowledge, experimental data on a ferromagnet in contact with other materials is still quite limited. A recent experiment<sup>30</sup> on Ta/CoFeB(1.0 nm)/MgO measured  $\mathbf{H}_R$  in FL-STT and found it to be about a factor of 4 smaller than the corresponding report on Pt/Co(0.6 nm)/AlO<sub>x</sub>.<sup>18</sup> A ferromagnetic metal in contact with topological insulators is an interesting combination to explore since topological insulators have strongly spin-orbit coupled states<sup>31</sup> near their surface. More experiments on various combinations are desired. For certain combinations of nonmagnetic metals [such as Bi/Ag (Ref. 29)], it is known that  $\alpha_R$  is drastically enhanced when atoms of neighboring layers get intermixed. A similar enhancement may occur in a ferromagnet in contact with heavy metals and may be responsible for the discrepancy between three experimental groups<sup>18,27,32</sup> on the values of  $\mathbf{H}_R$  in Pt/Co(0.6 nm)/AlO<sub>x</sub>. In particular, the experiment<sup>27</sup> found  $\mathbf{H}_R$  to be negligibly small but still observed anomaly (iii). It was argued that the

spin Hall effect (SHE) in the Pt layer converts an in-plane charge current to a perpendicular flow of a spin current, which generates the Slonczewski STT. Recalling the structural similarity between the Slonczewski STT and SL-STT, the magnetization switching can be explained by the SHE-induced Slonczewski STT. However, in the absence of FL-STT, the Slonczewski STT alone cannot generate anomalies (i) and (ii), as demonstrated in Figs. 3(c) and 3(d). Note that DW moves *along* the electron flow direction when  $j_e$  is large enough ( $>5 \times 10^{11}$  A/m<sup>2</sup>) and also that large enhancement of the DW speed does not occur.

To conclude, we demonstrated that RSOC generates two contributions (FL-STT and SL-STT) to STT and also that if RSOC is sufficiently strong, they can explain three anomalous features of the magnetization dynamics reported in an ultrathin magnetic system with structural symmetry breaking. This result will be useful for the development of next generation spintronic devices. During the preparation of this manuscript, we were made aware of work<sup>34</sup> which also derives SL-STT with similar results but does not discuss the implications of SL-STT on the anomalous DW motion.

We gratefully acknowledge M. D. Stiles, R. McMichael, and W. Rippard for valuable comments. This work was financially supported by the NRF (2010-0014109, 2010-0023798, 2011-0030784, 2011-0028163) and BK21. K.W.K. acknowledges financial support by the NRF (2011-0009278). K.J.L. acknowledges support under the Cooperative Research Agreement between the University of Maryland and the National Institute of Standards and Technology Center for Nanoscale Science and Technology, Award No. 70NANB10H193, through the University of Maryland.

\*kj\_lee@korea.ac.kr

†hwl@postech.ac.kr

<sup>1</sup>C. Chappert, A. Fert, and F. Nguyen Van Dau, *Nat. Mater.* **6**, 813 (2007).

<sup>2</sup>J. A. Katine and E. E. Fullerton, *J. Magn. Magn. Mater.* **320**, 1217 (2008).

<sup>3</sup>J. C. Slonczewski, *J. Magn. Magn. Mater.* **159**, L1 (1996).

<sup>4</sup>L. Berger, *Phys. Rev. B* **54**, 9353 (1996).

<sup>5</sup>M. D. Stiles and A. Zangwill, *Phys. Rev. B* **66**, 014407 (2002); K.-J. Lee, A. Deac, O. Redon, J.-P. Nozieres, and B. Dieny, *Nat. Mater.* **3**, 877 (2004); I. Theodonis, N. Kioussis, A. Kalitsov, M. Chshiev, and W. H. Butler, *Phys. Rev. Lett.* **97**, 237205 (2006).

<sup>6</sup>G. Tatara and H. Kohno, *Phys. Rev. Lett.* **92**, 086601 (2004).

<sup>7</sup>Y. Tserkovnyak, A. Brataas, and G. E. W. Bauer, *J. Magn. Magn. Mater.* **320**, 1282 (2008).

<sup>8</sup>S.-W. Jung, W. Kim, T.-D. Lee, K.-J. Lee, and H.-W. Lee, *Appl. Phys. Lett.* **92**, 202508 (2008); J. Ryu, S.-B. Choe, and H.-W. Lee, *Phys. Rev. B* **84**, 075469 (2011).

<sup>9</sup>S. Zhang and Z. Li, *Phys. Rev. Lett.* **93**, 127204 (2004).

<sup>10</sup>A. Thiaville, Y. Nakatani, J. Miltat, and Y. Suzuki, *Europhys. Lett.* **69**, 990 (2005).

<sup>11</sup>S. I. Kiselev *et al.*, *Nature (London)* **425**, 380 (2003); S.-C. Oh *et al.*, *Nat. Phys.* **5**, 898 (2009).

<sup>12</sup>S. S. P. Parkin, M. Hayashi, and L. Thomas, *Science* **320**, 190 (2008); T. Koyama *et al.*, *Appl. Phys. Express* **1**, 101303 (2008); L. Heyne *et al.*, *Phys. Rev. Lett.* **105**, 187203 (2010); T. Koyama *et al.*, *Nat. Mater.* **10**, 194 (2011); J. C. Lee, K. J. Kim, J. Ryu, K. W. Moon, S. J. Yun, G. H. Gim, K. S. Lee, K. H. Shin, H. W. Lee, and S. B. Choe, *Phys. Rev. Lett.* **107**, 067201 (2011); K.-J. Kim, J. Ryu, G. H. Gim, J. C. Lee, K. H. Shin, H. W. Lee, and S. B. Choe, *ibid.* **107**, 217205 (2011).

<sup>13</sup>M. Hayashi, L. Thomas, C. Rettner, R. Moriya, Y. B. Bazaliy, and S. S. P. Parkin, *Phys. Rev. Lett.* **98**, 037204 (2007); G. Meier, M. Bolte, R. Eiselt, B. Kruger, D. H. Kim, and P. Fischer, *ibid.* **98**, 187202 (2007).

<sup>14</sup>S. Ikeda *et al.*, *Nat. Mater.* **9**, 721 (2010).

<sup>15</sup>I. M. Miron *et al.*, *Nature (London)* **476**, 189 (2011).

<sup>16</sup>I. M. Miron *et al.*, *Nat. Mater.* **10**, 419 (2011).

<sup>17</sup>T. A. Moore *et al.*, *Appl. Phys. Lett.* **93**, 262504 (2008); T. A. Moore *et al.*, *ibid.* **95**, 179902 (2009).

<sup>18</sup>I. M. Miron *et al.*, *Nat. Mater.* **9**, 230 (2010).

<sup>19</sup>Y. A. Bychkov and E. I. Rashba, *J. Exp. Theor. Phys. Lett.* **39**, 78 (1984).

<sup>20</sup>K. Obata and G. Tatara, *Phys. Rev. B* **77**, 214429 (2008); A. Matos-Abiague and R. L. Rodríguez-Suárez, *ibid.* **80**, 094424 (2009).

- <sup>21</sup>A. Manchon and S. Zhang, *Phys. Rev. B* **78**, 212405 (2008); **79**, 094422 (2009).
- <sup>22</sup>J. Ryu, S.-M. Seo, K.-J. Lee, and H.-W. Lee, *J. Magn. Magn. Mater.* **324**, 1449 (2012).
- <sup>23</sup>The mechanism of this term is related to a mechanism discussed in the context of a perpendicular current [K. M. D. Hals, A. Brataas, and Y. Tserkovnyak, *Europhys. Lett.* **90**, 47002 (2010)].
- <sup>24</sup>S. Datta, *Electronic Transport in Mesoscopic Systems* (Cambridge University Press, Cambridge, UK, 1995).
- <sup>25</sup>When the conduction electron velocity is position dependent, the spin diffusion dynamics modifies the relation between the spin current and the electric field (Ref. 33) but it does not modify the RSOC-induced STTs expressed in terms of the current density.
- <sup>26</sup> $\alpha$  was reported (Ref. 18) to be about 0.5. We estimate  $\beta$  to be of order 0.1 from the reported (Ref. 15) magnitude of SL-STT. Incidentally, the estimation of  $\beta/\alpha$  from  $v_{\text{DW}}$  is incorrect since RSOC strongly modifies  $v_{\text{DW}}$ .
- <sup>27</sup>L. Liu, O. J. Lee, T. J. Gudmundsen, D. C. Ralph, and R. A. Buhrman, e-print arXiv:1110.6846.
- <sup>28</sup>J. Henk, M. Hoesch, J. Osterwalder, A. Ernst, and P. Bruno, *J. Phys.: Condens. Matter* **16**, 7581 (2004).
- <sup>29</sup>C. R. Ast, J. Henk, A. Ernst, L. Moreschini, M. C. Falub, D. Pacile, P. Bruno, K. Kern, and M. Grioni, *Phys. Rev. Lett.* **98**, 186807 (2007).
- <sup>30</sup>T. Suzuki *et al.*, *Appl. Phys. Lett.* **98**, 142505 (2011).
- <sup>31</sup>M. Z. Hasan and C. L. Kane, *Rev. Mod. Phys.* **82**, 3045 (2010).
- <sup>32</sup>U. H. Pi *et al.*, *Appl. Phys. Lett.* **97**, 162507 (2010).
- <sup>33</sup>K.-W. Kim, J.-H. Moon, K.-J. Lee, and H.-W. Lee, *Phys. Rev. B* **84**, 054462 (2011).
- <sup>34</sup>X. Wang and A. Manchon, *Phys. Rev. Lett.* **108**, 117201 (2012).